13th ewtec 2019
Proceedings of the 13th European Wave and Tidal Energy Conference 1-6 Sept 2019, Naples, Italy

# Global and regional tidal range resource

Simon P. Neill and Peter E. Robins

*Abstract*—**Although no tidal range power plant has been constructed for 25 years, the global resource is estimated to be around 1 TW. Recently, the concept of a tidal lagoon power plant has been actively pursued, considered to have lower environmental impact compared to existing barrage schemes. Here, we analyse a global tidal atlas, FES2014, to assess the magnitude and distribution of the tidal range resource. We also apply a higher resolution (ROMS) model to the northwest European shelf seas to assess the accuracy of the coarser (global) model. Excluding Hudson Bay, which is ice-covered for most of the year, and applying appropriate constraints, we find the global technical tidal range resource to be 14,075 TWh, equivalent to an annual mean power output of 1.61 TW. The majority of the resource is confined to a few shelf sea regions, including Australia (mainly Western Australia), Canada (Fundy), the UK, and France. We examine two contrasting regions in more detail: the Patagonian region of Argentina, and Western Australia, discussing challenges and opportunities for grid integration. Finally, we find that the global model overestimates the tidal range resource of the northwest European shelf seas by around 14% compared to the high resolution (ROMS) model of the region, and we present and discuss the distribution of the resource estimated by the two models.**

*Keywords*— **Tidal barrage, Tidal energy, Tidal lagoon, Tidal range**

## I. Introduction

FOR centuries, the potential energy of the tides has been converted into other useful forms of energy. Tide mills have a history extending back to the 6th Century, and were a common site along the western seaboard of Europe during medieval times, particularly along the coasts of Portugal, northern Spain, France, and the south coast of England (English Channel) [1]. More recently, in the second half of the 20th Century, tidal range power plants, generating electricity from tidal range, have been developed, and there are currently 5 of these power plants in operation (Table I). All of these tidal range power plants are barrages, which are generally associated with significant environmental impacts, particularly for larger schemes [2]. A more recent concept, considered to have lower environmental impact [3], is a tidal lagoon; however, no lagoon project has yet proceeded to the construction phase, and indeed no tidal range power plant of any type has been constructed in the last 25 years, primarily due to high capital costs.

Despite the lack of progress in developing the tidal range resource (e.g. a globally installed capacity of 520 MW – Table I), it has been suggested that the global potential is around 1 TW [4]. Here, we analyse a global tidal atlas, FES2014 [5], to refine this estimate, particularly within the constraints of likely water depths suitable for construction of the embankment (generally < 20 m, and certainly < 30 m), beyond which projects would be unfeasible. We examine several regions in more detail, including the Patagonian region of Argentina, western Australia, and the northwest European shelf seas. We also apply a higher resolution model to the latter region to assess the accuracy of the global model assessment, resulting in guidance on the model resolution that is necessary to accurately quantify the tidal range resource.

## II. Methods

### A. Sources of data

For the global analysis of the tidal range resource, the FES2014 tidal dataset was used, which provides tidal elevations (amplitude and phase) for 34 tidal constituents at a consistent 1/16° × 1/16° global resolution. Water depths were taken from the GEBCO-2014 gridded bathymetry dataset, available on a 1/120° × 1/120° global grid (which was resampled here to a 1/16° × 1/16° grid to match the FES2014 grid points), and referenced to mean sea level.

For more detailed examination of the northwest European shelf seas, the 3D ROMS model (Regional Ocean Modeling System) was applied (see Section B). The model bathymetry for this region was again interpolated from GEBCO, and the boundary conditions from TPX07 global tidal dataset at 1/4° resolution [6].

TABLE I
CHARACTERISTICS OF EXISTING TIDAL BARRAGE SCHEMES

| Power plant | Year | Capacity (MW) | Basin area (km²) | Operation mode |
|---|---|---|---|---|
| La Rance, France | 1966 | 240 | 22 | Two-way with pumping |
| Kislaya Guba, Russia | 1968 | 1.7 | 2 | Two-way |
| Annapolis Royal Generating Station, Canada | 1984 | 20 | 6 | Ebb only |
| Jiangxia, China | 1985 | 3.9 | 2 | Two-way |
| Lake Sihwa, Korea | 1994 | 254 | 30 | Flood only |

Paper ID number: 1363; Conference track: Tidal resource characterization.
S.P. Neill and P.E. Robins are at the School of Ocean Sciences, Bangor University, Menai Bridge, UK LL59 5AB (email: s.p.neill@bangor.ac.uk)

  

### B. ROMS model

The model domain of the northwest European shelf seas extended from 14° W to 11° E, and from 42° N to 62° N. The domain was discretized in the horizontal using a curvilinear grid, applying a fixed longitudinal resolution of 1/60°, and a variable latitudinal resolution of 1/128° to 1/81° (~0.9 to 1.4 km) to preserve the cell aspect ratio. The vertical model grid consists of 10 layers distributed according to the ROMS terrain-following coordinate system. The open boundaries of the model were forced by tidal elevation (Chapman boundary condition) and tidal velocities (Flather boundary condition), generated by 10 tidal constituents (M2, S2, N2, K2, K1, O1, P1, Q1, Mf, and Mm) obtained from TPX07. The validation procedure for elevations, based on harmonic analysis performed at 20 tide gauges distributed throughout the model domain, produced scatter indices (SI)[1] of 8% and 6% for M2 and S2 amplitudes, respectively. Further information about the model configuration and validation can be found in Robins et al. [7]. Tidal analysis from a 30-day simulation was used to calculate the following 5 dominant tidal constituents, which were used to construct annual elevation time series at each model grid cell: M2, S2, N2, K1, and O1.

### C. Calculation of tidal range resource

The calculated resource assessment is based on water depth and a constructed annual sea surface elevation signal. For each model grid cell, an annual elevation time series was constructed (using T_TIDE [8]), based on the following 5 tidal constituents: M2, S2, N2, K1, and O1. For each time series, the tidal range ($H$) of consecutive rising and falling tides was calculated, allowing the annual potential energy ($PE$, per m²), to be calculated as follows:

$$PE = \sum_{i=1}^{n} \frac{1}{2} \rho g H_i^2 \quad (1)$$

where the subscript $i$ denotes each successive rising and falling tide in a year ($n$~1411 in regions where the tides are semidiurnal), ρ is the density of seawater, and $g$ is acceleration due to gravity.

Some assumptions have been made about areas that are suitable for tidal range developments, and we have calculated how much energy there is in just these areas. The true limit of any development will be when the energy yield does not increase the financial return sufficiently compared with the development and running costs [9]. Here, we assume a minimum acceptable annual energy yield of 50 kWh/m² (based on the energy yield from a constant tidal range of 5 m), and also a maximum water depth of 30 m (since construction costs of the embankment would likely be prohibitive in deeper waters).

## III. Results

### D. Global results (FES2014)

The global distribution of the tidal range resource (Fig. 1) shows how the resource is concentrated in a few key regions, particularly Hudson Bay, the Atlantic coast of Patagonia, the northwest European shelf seas, and Western Australia. Since Hudson Bay is ice-covered for much of the year, we exclude this region from our analysis.

By assuming a minimum energy density of 50 kWh/m² and constraining water depths to < 30 m, the global annual tidal range resource is 14,075 TWh (equivalent to an annual mean power output of 1.61 TW), distributed across eleven countries (Table 2).

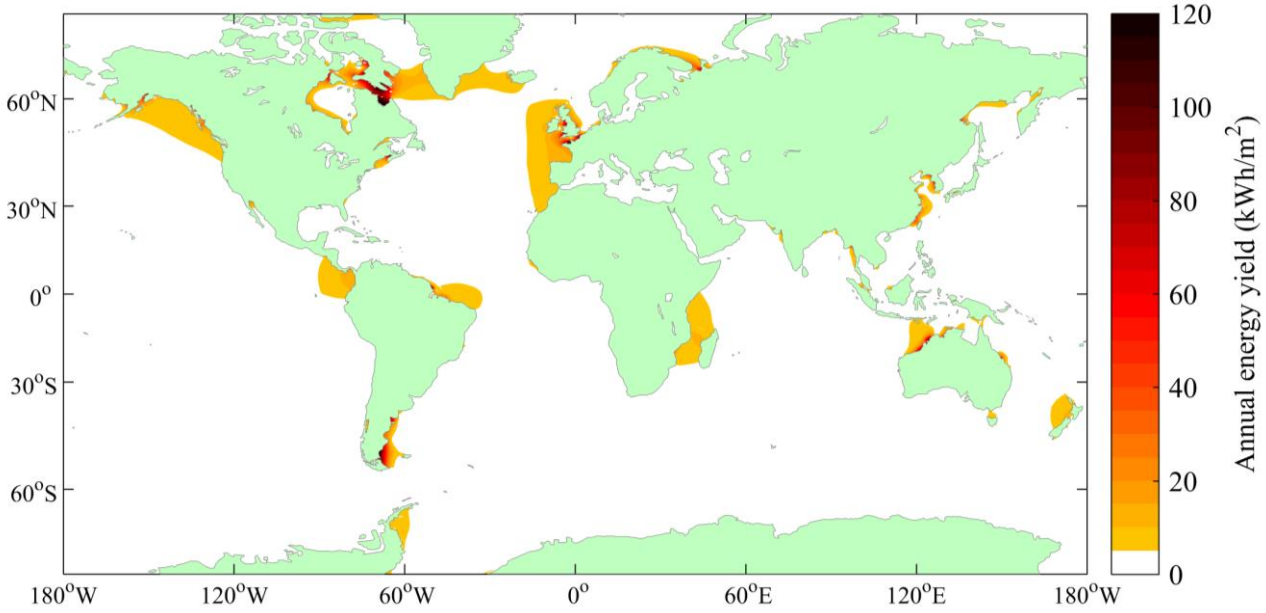


*Fig. 1. Global tidal range resource without bathymetric constraints.*

[1]Scatter Index is the Root-Mean-Square-Error normalized by the mean of the observations.

TABLE II
ANNUAL POTENTIAL ENERGY PER COUNTRY

| Country | Annual P.E. (TWh) | Annual mean power (GW) |
|---|---|---|
| **Global** | **14075** | **1607** |
| Australia | 4277 | 488 |
| Canada (Fundy) | 3298 | 376 |
| UK | 1784 | 204 |
| France | 1779 | 203 |
| US (Alaska) (partial sea ice) | 1504 | 172 |
| Brazil | 724 | 83 |
| South Korea | 260 | 30 |
| Argentina | 151 | 17 |
| Russia (NW) (partial sea ice) | 102 | 12 |
| Russia (NE) (partial sea ice) | 80 | 9 |
| India | 46 | 5 |
| China | 29 | 3 |

### E. *Regional results (FES2014)*

We present more detailed results, from the global model, for Patagonia (Fig. 2) and Western Australia (Fig. 3). Presentation of the northwest European shelf seas is reserved for Section F, since examination of this region forms the basis of validation between global and regional modelling scales.

There is an extensive region of the Atlantic coast of Patagonia where the annual energy density exceeds 120 kWh/m², in the Bahia Grande (Fig. 2). Although the high energy region in the north of the Bahia Grande is dominated by the Parque Nacional Monte Leon[1], and so opportunities for coastal development may be limited, the region to the south of the bay is promising, and includes relatively large populations, for example Rio Gallegos (population 96,000), in a region that is beyond the reach of the electricity grid that is concentrated in the north of Argentina (and extends no further south than the southern part of the Golfo San Jorge). There is a further region to the north (Golfo San Matias) where the annual energy density is lower, at around 70 kWh/m², but with more opportunities for grid connectivity, including access to a 330 kV east/west connection to Chile.

There are extensive regions of Western Australia where the tidal energy density exceeds 50 kWh/m² (Fig. 3). Although the population density along Eighty Mile Beach and to the north of Broome is low (e.g. Port Hedland, population 14,000; Broome, population 15,000), there is access to a localized transmission grid around Port Hedland. Further northeast from Eighty Mile Beach, there is little electricity infrastructure south of Darwin. There is a project (currently delayed) to construct a 40 MW barrage across Doctor's Creek, near Derby, where the density of the tidal range resource is around 50 to 60 kWh/m².

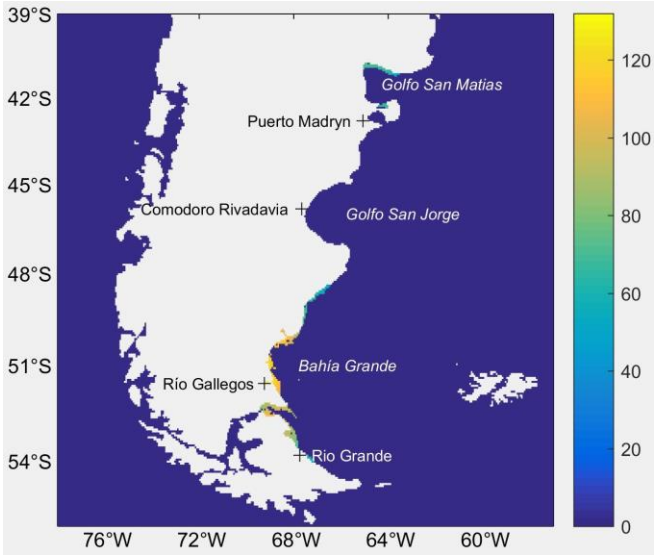


*Fig. 2. Tidal range resource in Patagonia (annual energy yield in kWh/m²), assuming a minimum depth of 30 m for construction of embankments.*

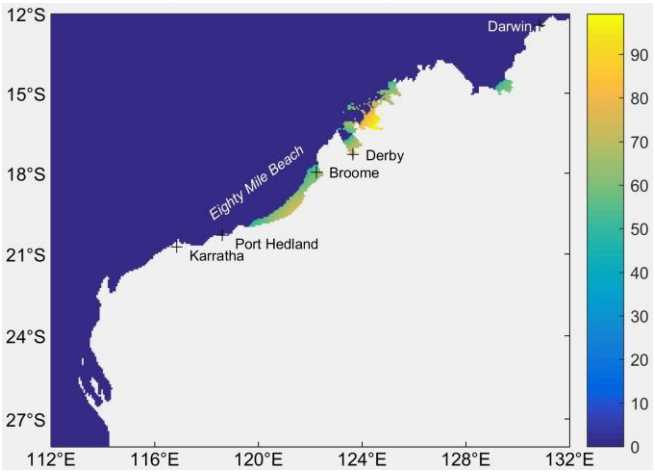


*Fig. 3. Tidal range resource in Western Australia (annual energy yield in kWh/m²), assuming a minimum depth of 30 m for construction of embankments.*

### F. *Regional results (ROMS)*

To confirm the accuracy of the regional tidal range resource assessments that were based on the global tidal database (FES2014), we examined a much researched case study, the northwest European shelf seas, in more detail by applying the ROMS model (Section B) at higher resolution (~1 km resolution, in comparison to the FES2014 resolution of ~7 km).

Analysis of the tidal range resource over the northwest European shelf seas, based on the ROMS model and assuming (a) a minimum water depth of 30 m to construct the embankment, and (b) a minimum energy density of 50 kWh/m², leads to an annual potential energy estimate of

[1] Home to many coastal/marine species, including sea lions, southern right Whales, and Magellanic penguins

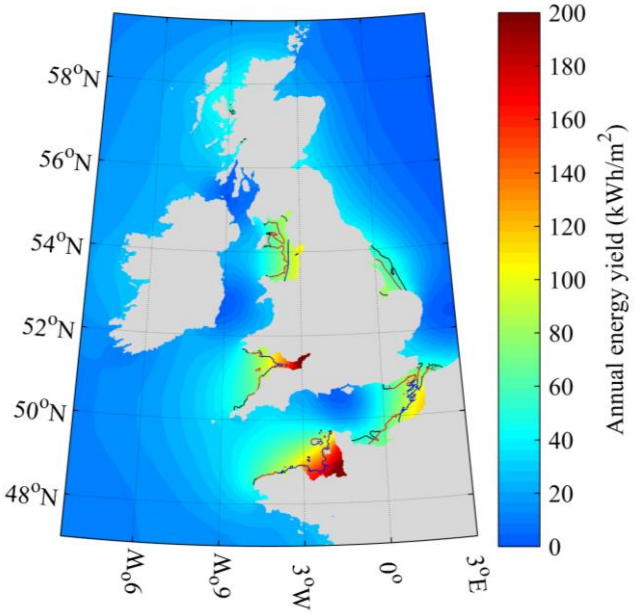


*Fig. 4. The theoretical tidal range energy resource over the northwest European shelf seas, calculated as annual energy density (kWh/m²). Areas landward of the [blue, red, black] contour lines denote regions with water depths less than 30 m and where energy density exceeds 84, 60, and 50 kWh/m², respectively.*

3064 TWh – a reduction of 14% compared to analysis based on the coarser (FES2014) model (Section D). If the minimum energy density is increased to either 60 or 84 kWh/m², the resource reduces to 2804 and 2022 TWh, respectively (Table III) [1]. Note that the sea space available for tidal range projects (shown as the regions landward of the contour lines on Fig. 4), approximately halves from 31,415 km² to 15,813 km² when the threshold energy density is increased from 50 to 84 kWh/m² (Table III).

To further investigate variations in the potential energy estimates between the two model resolutions and formulations, we examined the distribution of the energy density produced by FES2014 and ROMS (Fig. 5). There are very obvious differences between the two distributions, with significant over-estimates of the area of 'lower' energy regions (50-70 kWh/m²) by FES2014. Due to increased model resolution (~1 km compared to ~7 km), the ROMS simulation was better able to resolve very high energy regions (> 150 kWh/m²), such as the upper reaches of the Bristol Channel, and so one wonders what the implications of refined model resolution would be on the potential energy estimates of the Patagonian shelf and

TABLE III
ANNUAL ENERGY OUTPUT AND SEA SPACE FOR NW EUROPEAN SHELF SEAS FOR VARYING ENERGY DENSITY THRESHOLDS

| Min. energy density (kWh/m²) | Annual energy output (TWh) | Sea space (km²) |
|---|---|---|
| 50 | 3064 | 31,415 |
| 60 | 2804 | 26,682 |
| 84 | 2022 | 15,813 |

[1] 84 kWh/m² corresponds to the potential energy of the proposed Swansea Bay tidal lagoon

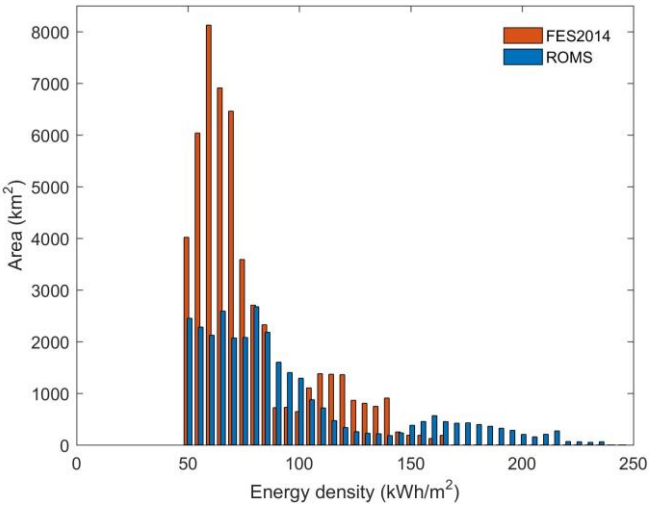


*Fig. 5. Distribution of calculated tidal range energy density for the northwest European shelf seas between global (FES2014) and regional (ROMS) model configurations.*

Western Australia, presented in Section E. Finally, there was little available sea space/resource over the northwest European shelf seas at the 120-150 kWh/m² threshold, as further demonstrated in Fig. 6. It is suspected that water depths within these energy density levels exceed 30 m, and hence would not be suitable for development of tidal range projects. The regions of very high energy density (> 150 kWh/m²) are associated with the upper reaches of the Bristol Channel and Mont Saint Michel Bay, both regions that are characterized by significant inter-tidal areas, and therefore challenging to exploit.

## IV. DISCUSSION

Our simulations demonstrate that reducing model resolution from ~7 km to ~1 km leads to a 14% reduction in the estimated tidal range resource over the northwest European shelf seas. However, we have not compared similar model setups; for example, the FES2014 global model is based on an unstructured grid and incorporates data assimilation, whereas ROMS is based on a structured grid and is a forward stepping model. Further, the

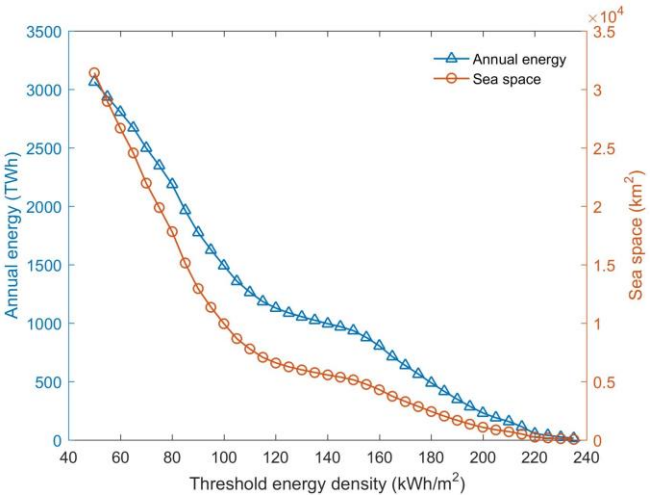


*Fig. 6. Annual energy output and sea space for a range of energy density thresholds, northwest European shelf seas.*

boundary conditions of the ROMS model (TPX07) are inconsistent with the global model. Therefore, a systematic approach would maintain model configurations, but successively refine model resolution until convergence. It is also important to point out that our ROMS application was based on a minimum water depth of 10 m to prevent model cells from 'drying out', and a thorough model application would incorporate alternate wetting and drying, which is particularly relevant in regions such as the upper reaches of the Bristol Channel that are characterized by high tidal range and extensive inter-tidal areas. Finally, the resolution of the bathymetry used here (GEBCO) is around 930 m, and so a higher resolution bathymetry dataset (e.g. multibeam survey) would be required if model resolution were refined beyond 1 km.

## ACKNOWLEDGEMENT

FES2014 data was provided by AVISO, and GEBCO data from the British Oceanographic Date Centre (BODC).

## REFERENCES

[1] T. McErlean and N. Crothers, Harnessing the Tides, The Early Medieval Tide Mills at Nendrum Monastery, Strangford Lough, Northern Ireland. Archaeological Monographs No 7. TSO, 1997.

[2] C. Retiere, "Tidal power and the aquatic environment of La Rance," *Biol. J. Linn. Soc.*, vol. 51, pp. 25-36, 1994.

[3] C. Hendry, The Role of Tidal Lagoons – Final Report, 2017.

[4] A. Lewis, S. Estefen, J. Huckerby, W. Musial, T. Pontes, and J. Torres-Martinez, "Ocean energy", in *IPCC Special Report on Renewable Energy Sources and Climate Change Mitigation*, pp. 497-534, 2011.

[5] L. Carrere, F. Lyard, M. Cancet, and A. Guillot, 2015, "FES 2014, a new tidal model on the global ocean with enhanced accuracy in shallow seas and in the Arctic region," in *EGU General Assembly Conference Abstracts*, vol. 17, 2015.

[6] G.D. Egbert and S.Y. Erofeeva, "Efficient inverse modeling of barotropic ocean tides," *J. Atmos. Ocean. Tech.*, vol. 19, pp. 183-204, 2002.

[7] P.E. Robins, S.P. Neill, M.J. Lewis, and S.L. Ward, "Characterising the spatial and temporal variability of the tidal-stream energy resource over the northwest European shelf seas," *Appl. Energ.*, vol. 147, pp. 510-522, 2015.

[8] R. Pawlowicz, B. Beardsley, and S. Lentz, "Classical tidal harmonic analysis including error estimates in MATLAB using T_TIDE," *Comput. Geosci.*, vol. 28, pp. 929-937, 2002.

[9] S.P. Neill, A. Angeloudis, P.E. Robins, I. Walkington, S.L. Ward, I. Masters, M.J. Lewis, M. Piano, A. Avdis, M.D. Piggott, G. Aggidis, P. Evans, T. Adcock, A. Zidonis, R. Ahmadian, and R. Falconer, "Tidal range energy resource and optimization–Past perspectives and future challenges," *Renew. Energ.*, vol. 127, pp. 763-778, 2018.